

Simultaneous measurement of velocity and temperature field of high temperature jet using thermographic phosphor particles

Dong Kim¹, Seung Jae Yi², Hyun Dong Kim¹, Kyung Chun Kim^{1,*}

¹School of Mechanical Engineering, Pusan National University, Busan, Korea

²Propulsion Test and Evaluation Team, Korea Aerospace Research Institute, Daejeon, Korea

*corresponding author: kckim@pusan.ac.kr

Abstract In order to overcome existing complicated and costly simultaneous measurement system, an inexpensive and simple measurement system was suggested to measure the temperature field and velocity field at high temperature. The manganese-activated magnesium fluorogermanate ($Mg_4FGe_6:Mn$, MFG) which is one of thermographic phosphor with luminescence characteristic of excitation at 385 nm wavelength and emission 660 nm wavelength light was used as a tracer particle for PIV. Instead of costly Nd:YAG laser, Light Emitting Diode (LED) which is relatively inexpensive and alterable in terms of wavelength and only one high speed camera with CMOS sensor were used for the simultaneous measurement system. To validate the constructed simultaneous measurement system, dispersion of the confined oil jet with high temperature was investigated. The instantaneous temperature and velocity field were obtained when 200 °C of silicon oil was injected into the 25 °C of the silicon oil chamber. For the temperature field analysis, the decay – slope method was used, and the velocity field was obtained by two-frame cross correlation algorithm. The instantaneous temperature and velocity field were obtained successfully with 0.1 second time interval. It is investigated that the velocity of injected silicon oil was rapidly decreased because of the change of viscosity of silicon oil over temperature. And the injected high temperature silicon oil was cooled by surrounding low temperature silicon oil. Therefore, the velocity of oil jet was decreased rapidly and was dispersed widely. The temperature gradient is also related to oil jet dispersion. The temperature difference before and after of a dispersion point appears significantly, since the temperature of silicon oil difference between the spread widely area and non-spread area. The temperature field and velocity field were obtained successfully by simple simultaneous measurement system using thermographic phosphor tracer.

Keywords: Simultaneous measurement, Thermographic phosphor, Light Emitting Diode, Temperature field, Velocity field, Particle Image Velocimetry

1 Introduction

To analyze the phenomena of fluid machinery or other engineering flows, measurements of the physical parameters are the first step of analysis. Temperature is one of the important physical parameters of flow phenomena in addition to velocity, and measurement techniques for these parameters have developed rapidly over the last few decades. The PIV (Particle Image Velocimetry) technique makes it possible to measure the velocity field [1]. Temperature can also be used to provide field information using thermal paint and phosphor thermometry techniques. On the other hand, the disadvantages of thermal paint, which is expensive and requires skill and experience, have led many researchers to focus on improving the phosphor thermometry technique [2-6]. Thermographic phosphors have been used to measure temperature since the late 1930s [3], and they have been applied to a range of application fields. Phosphor thermometry techniques are also applied to measure the temperature of internal combustion engines and single droplets [4-6]. However, these two-dimensional measurement techniques could provide only one physical parameter. In the case of transient phenomena, simultaneous multi-physics measurement is important to analyze the correlations between more than two physical parameters. It is difficult to apply simultaneous measurement with conventional measurement techniques, but optical measurement techniques allow for multi-physics measurement at the same time. For simultaneous multi-physics measurement, functional particles which are sensitive to temperature could be used. These functional particles could be used in PIV experiments as tracers, and the change of phosphorescence characteristics such as lifetime or emission shift could be converted to other physical information. A few researchers conducted simultaneous measurement of temperature-velocity field at high temperature directly using thermographic phosphor. Fond et al. conducted simultaneous measurement of temperature-velocity field using BAM:EU phosphor [7]. They used BAM:EU particle and Al_2O_3 particle simultaneously and also used aligned 3rd harmonic of an Nd:YAG laser and

another 532nm Nd:YAG laser on the measurement section in order to excite each particle. An interline transfer CCD camera was used to measure PIV and two non-intensified CCD camera were used for intensity ratio-based analysis to obtain temperature. Using such measurement system, they measured velocity field and temperature field of 550K gas jet with temperature accuracy 2% and precision between 2 and 5%. Such measurement system has high accuracy to measure temperature field and velocity field at high temperature. However, it needs high cost investment to organize measurement system including 3 costly CCD cameras and more than two Nd:YAG lasers which are expensive lighting devices. In addition to this, optically precise setting is required, because different lasers and detectors are used.

In this study, in order to overcome the existing complicated and costly measurement system, an inexpensive and simple measurement system was suggested to measure temperature field and velocity field at high temperature in this thesis. Instead of costly Nd:YAG laser, Light Emitting Diode (LED) which is relatively inexpensive and alterable in terms of wavelength and only one high speed camera with CMOS sensor were used. With these as simultaneous measurement system of temperature field and velocity field at high temperature using optical property of phosphor, temperature field and velocity field of oil jet were measured at high temperature range.

2 Thermographic phosphor

There are a variety of thermographic phosphors, so proper thermographic phosphor needs to be selected depending on the range of measure temperature and analysis method. In this study, Mg₄FGeO₆:Mn (MFG) is selected as thermographic phosphor, because it has relatively continuing characteristic of phosphorescence while it can measure at a wide range of temperature [8]. Manganese ion absorbs ultraviolet range of 385 nm and emits fluorescence of 650 nm wavelength. Figure 1 shows the absorption and emission spectra of MFG.

2.1 Decay-slope analysis method

Generally, intensity based method and temporal signal based method are used as one of the temperature field analysis method using thermographic phosphors. Absolute intensity method is analysis method based on the characteristic of changing fluorescence intensity depending on the concentration of quencher, but it needs to be controlled, because signal can be differ by other factors such as uniformity of illumination, concentration of phosphor. Compared to absolute intensity method, intensity ratio method has higher accuracy, but its measurement system is complicated.

Temporal signal based method is analysis method using characteristic of emission of phosphor with time, and lifetime analysis and rise-time analysis are generally used. Compared to intensity method, temporal signal based method has higher accuracy, but it takes long time to analyze [9]. In this regards, Yi et al. suggested decay-slope analysis method as a new analysis method using temporal signal [10], and it is based on the phosphorescence signal with time in equation (1).

$$V(t) = Ae^{t/\tau} + b + \varepsilon(t) \quad (1)$$

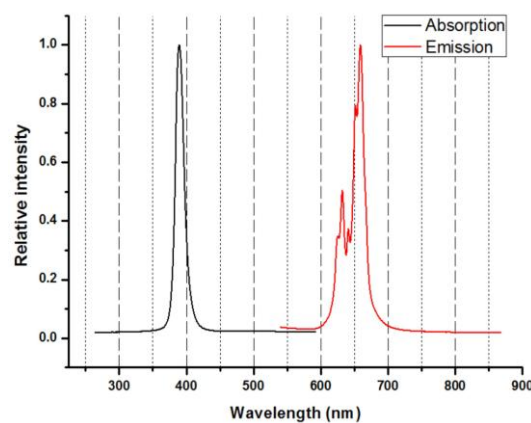


Fig. 1 Absorption and emission spectra of MFG

where A and b are the initial intensity and baseline offset, τ and t are the lifetime and time, and $\varepsilon(t)$ is noise term generated by shot noise, quantization noise and background radiation. The noise term $\varepsilon(t)$ can be reduced by averaging repeated experiments, and in case of be known baseline term (b) a priori, equation 1 can be rewritten as

$$I(t) = Ae^{-t/\tau} \quad (2)$$

where $I(t)=V(t)-b$. The normalized intensity which was obtained by intensity $I(t)$ divided by initial intensity (I_0) can eliminate the some error terms, such as non-uniform light source/phosphor concentration and shot-to-shot fluctuation.

$$I(t)/I_0 = A'e^{-t/\tau} \quad (3)$$

The phosphorescence lifetime could be estimated using nonlinear least-squares approximation algorithm to the equation 3, respectively. The Trust-Region algorithm was used to obtain the lifetime constant, and lifetime constant is consisted by decay constant (λ)

$$\lambda = 1/\tau \quad (4)$$

Equation (3) can be summarized by decay slope constant λ and log-scale term

$$I(t)/I_0 = A'e^{\lambda t} \quad (5)$$

$$\ln(I_0/I(t)) = \lambda t + \ln(A') \quad (6)$$

where λ and A' could be estimated using linear least-squares curve fitting. According to equation (6), the ratio of intensity between I_0 and $I(t)$ and time t has a linear relationship with the slope of decay constant λ .

3 Experimental setup and calibration

Figure 2 (a) is the experimental setup to acquire the calibration curve of simultaneous measurement of temperature and velocity field using MFG particles. Temperature of working fluid that is mixed with silicon oil and MFG particles was controlled by the hot plate. Working fluid was delivered into the channel for calibration by an oil pump (DPO 15N-220, Daehwa pump co.) and the fluid that passed the test section was collected using a beaker. Moreover, all pipes were insulated until the fluid was entering into the channel for minimizing heat loss. The temperature just before the nozzle into the channel was monitored by using a K-type thermocouple. To illuminate the manganese ion in MFG, an ultraviolet LED (Prizmatix, UHP-T-LED-385), which has around 0.2 mJ per pulse and 385 nm wavelength was used. The phosphorescence image from thermographic phosphor was obtained using a high speed camera (Photron SA 1.1) with 8000 frame per second. A narrow band-pass filter around 655 nm wavelength (Edmundoptics, #67-051) was mounted on a 50 mm lens (Canon 50 mm f/1.2) to obtain only the luminescence signal. A function generator was used to control the start timing of the UV-LED and high speed camera. Therefore, the distribution of instantaneous temperature with 0.1 second interval is quantitatively measured with this experimental setup. Figure 2 (b) shows the channel and its size used for calibration and the location of field of view. Using tempered glass, the square chamber with the size of 100 mm x 60 mm x 3 mm was fabricated and two slit nozzles whose size of 2 x 20 mm were installed at the inlet and outlet of the chamber. Phosphorescence images to obtain the calibration curve using the decay slope analysis method were acquired in the region just after the inlet nozzle of the test section, so that the difference of temperature could be minimized and temperature of the working fluid was measured by thermocouple. Figure 3 (a) shows the phosphorescence image obtained in the calibration test at 20 °C. The image was measured by 640 pixels by 816 pixels. Decay slope constants were extracted using the decay slope algorithm, and Figure (b) shows calculated distribution of decay slope. The decay slop is around 0.28 at 20 °C. With this process, the calibration test was continued up to 210 °C and Figure 4 is obtained as a result. The result of calibration test shows that as temperature is higher, the value of decay slope increases. Comparing this result with the result in our previous work on and the result from

Brubach et al. [8], it is confirmed that all results agree well each other for the same range of temperature.

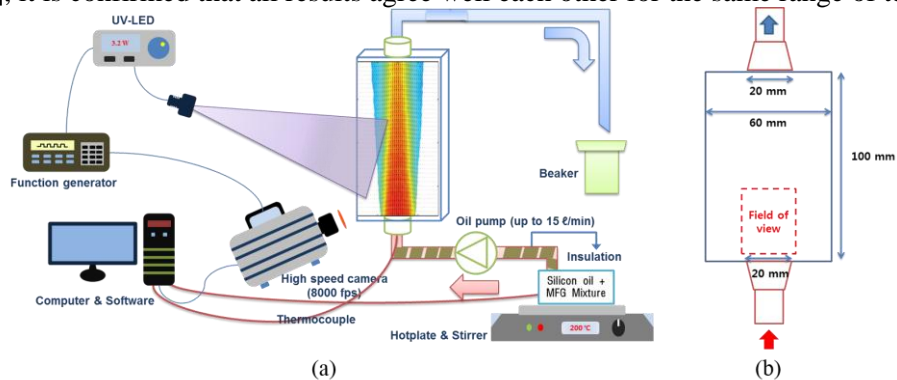


Fig. 2 Experimental apparatus; (a) Setup for calibration, (b) Tempered glass chamber for calibration

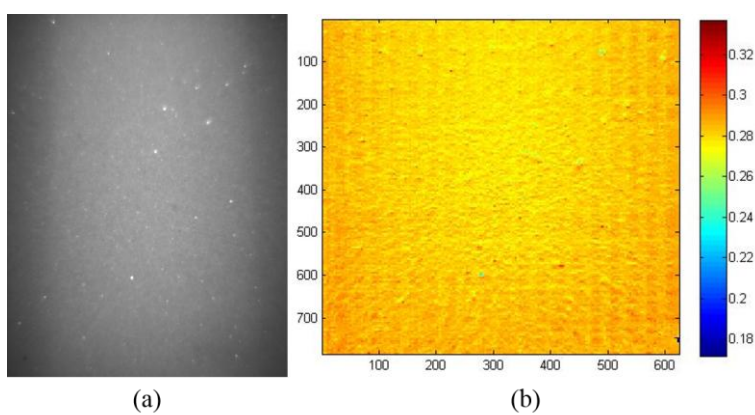


Fig. 3 Calibration tests; (a) Phosphorescence image at 20 °C, (b) Decay slope distribution at 20 °C

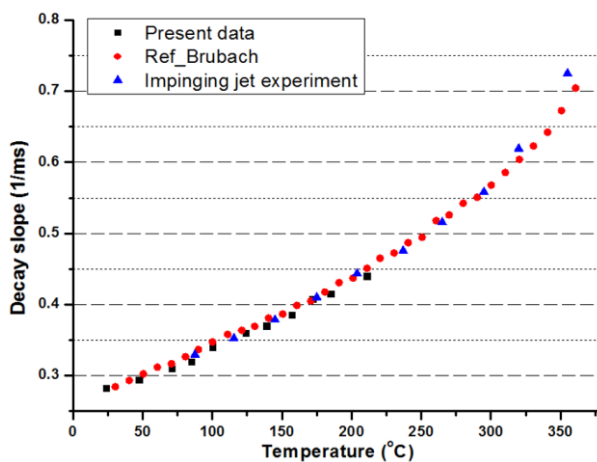


Fig. 4 Comparison of calibration results

Figure 5 shows the size of chamber and nozzle used for experiment and the field of view for simultaneous measurement of temperature field and velocity field. For oil jet, mixture of silicon oil and MFG particle as working fluid that is same as in calibration test, overall experimental setup is nearly similar to that of the calibration test, but the size of chamber and nozzle were changed. The test chamber was filled with silicon oil with MFG particles and the initial temperature was 20 °C.

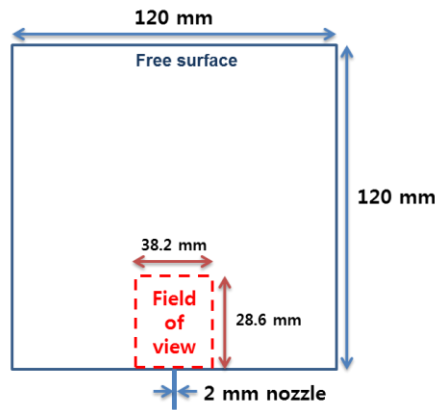


Fig. 5 Details of flow chamber and field of view

4 Results and discussion

Figure 6 (a) is one of image of phosphor particles used in the data analysis. It shows that the jet issues from the bottom of the center and the phosphorescence intensity of oil jet with MFG particles is relatively lower than that of the surroundings. This can be explained by the characteristics that as the temperature is higher, luminescent intensity is lower. Therefore, as the jet proceeds the temperature of jet is getting lower and lower followed by its phosphorescence intensity is nearly similar to that of the surrounding fluid at the center of the image. Figure 6 (b) is ensemble averaged velocity fields obtained with 300 instantaneous velocity fields from the two-frame cross correlation PIV algorithm. It is interesting to note that the velocity of oil jet decreases significantly when the hot oil jet is reached in cold surroundings. The main reason is conjectured to the viscous drag due to huge increase of dynamic viscosity with decrease of temperature. The peak speed of center of jet is up to 0.45 m/s and surroundings of jet is about 0.03 m/s.

Figure 7 shows velocity and temperature field applying the calibration curve obtained in calibration test and the decay slope algorithm with measured experimental data. Temperature is under around 120 °C at $Y/D_N < 5$ where flow recirculates but temperature is generally higher towards flow direction at the range of $Y/D_N > 5$ where jet spreads.

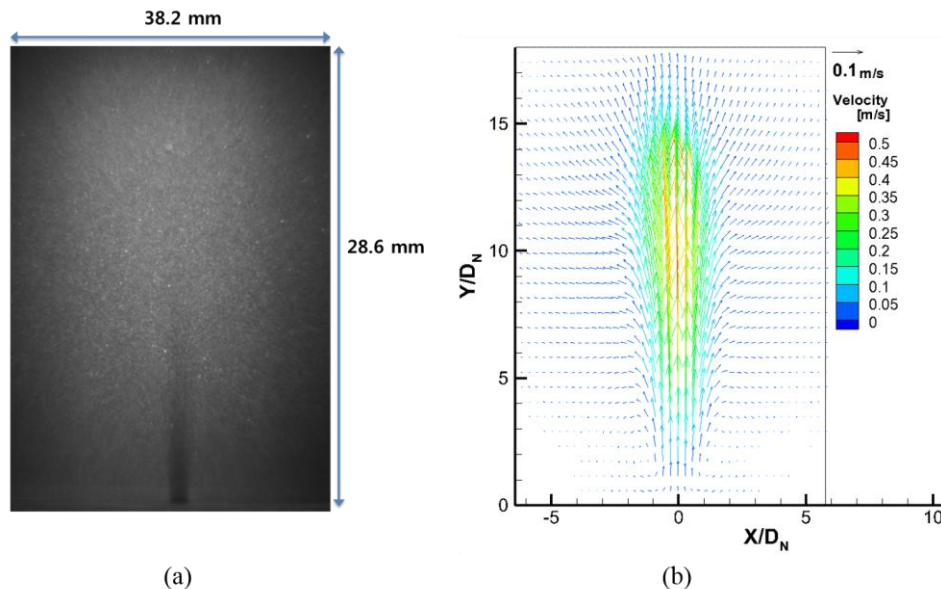


Fig. 6 Simultaneous measurements of high temperature oil jet; (a) Obtained image for simultaneous measurement, (b) Ensemble averaged velocity distribution

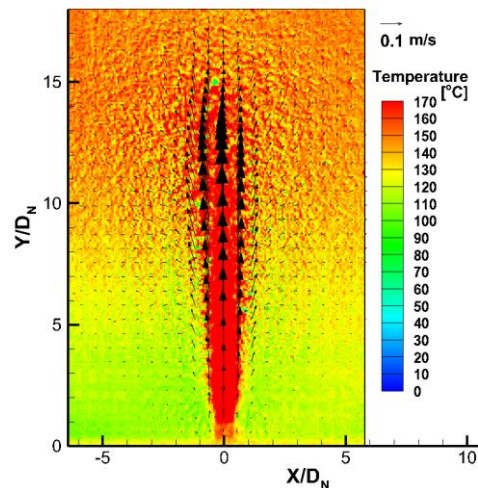


Fig. 7 Result of simultaneous measurement of velocity and temperature field

According to the velocity data from PIV analysis, the phosphor particles on the oil jet moves 10 pixels per 1 ms, therefore, the maximum distance of particle movement is up to 50 pixels when one phosphor signal obtained for phosphor thermometry. However, the phosphorescence signal in the small interrogation window of 4 x 4 pixels is considered in the temperature field data analysis in Figure 7, it is hard to fully consider such movement of particle and it results in analysis errors. In order to reduce analysis errors caused by movement of particle, the size of interrogation window is adjusted. As selecting the bigger interrogation window, analysis errors caused by particle movement is reduced, but the spatial resolution of temperature tends to be lower. In order to improve this, the interrogation window for PIV was set to 16 x 16 pixels and the phosphorescence signal of 48 x 48 pixels which is three times bigger than the original size of interrogation window for temperature measurement was considered for data analysis and its result is shown in Figure 8. Compared to the previous result obtained by 4 x 4 interrogation window in Figure 7, the spatial resolution is decreased but overall temperature distribution is similar. In order to check temperature distribution at the center of the jet, the temperature distribution at $X/D_N = 0$ was extracted and compared to the result shown in Figure 7. Figure 9 shows the temperature distribution at the center of jet, according to the different size of interrogation window. According to the line data, two results are in the similar range at $Y/D_N > 8$, and considering relatively larger interrogation window, deviation of temperature data decreases. The temperature distribution of 16 x 16 interrogation window with considering 48 x 48 pixels to obtain phosphorescence signal in the jet shows around 200 °C and it is almost same with the initial temperature of silicon oil jet. However, the results of temperature obtained by smaller interrogation window shows the temperature along the centerline reaches over than 350 °C, which is unrealistic because of the particle missing. The effect of particle movement had been removed by replacing larger interrogation window. Therefore, the size of interrogation window should be considered carefully according to the velocity of phosphor particles to obtain more accurate result.

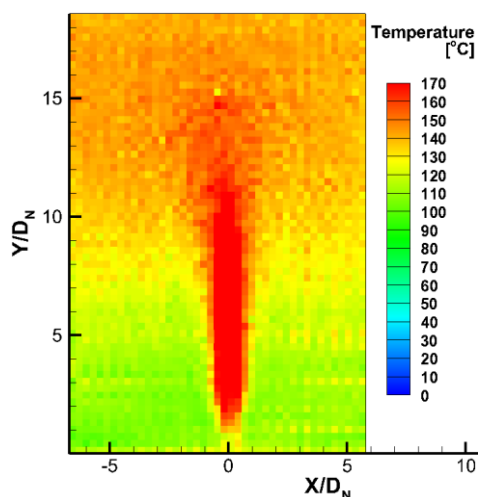


Fig. 8 Temperature field by 16 x 16 interrogation window

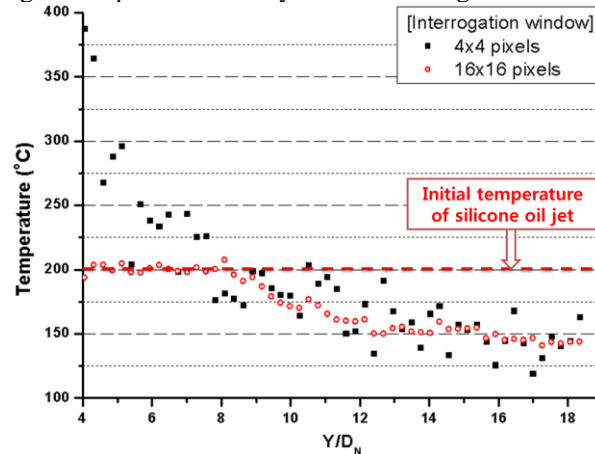


Fig. 9 The comparison of line data at X/D_N = 0

5 Conclusions

In this study, the simultaneous measurement technique using one light source and one high speed camera were developed and the simultaneous measurement of instantaneous temperature and velocity fields at 200 °C were conducted with Mg₄FGeO₆:Mn particles. The effects of phosphor particle movement were analyzed with the size of interrogation window to obtain accurate data. It is found that there exist a suitable interrogation window size and velocity of flow for simultaneous measurement of velocity and temperature field with high accuracy. Therefore, two dimensional measurement of temperature and velocity distribution were successfully obtained.

ACKNOWLEDGEMENT

This work was supported by the Energy Efficiency & Resources Core technology Program of the Korea Institute of Energy Technology Evaluation and Planning (KETEP) granted financial resource from the Ministry of Trade, Industry & Energy, Republic of Korea (No. 20132020000390).

References

- [1] R. J. Adrian (1984) Scattering Particle Characteristics and Their Effect on Pulsed Laser Measurements of Fluid-Flow-Speckle Velocimetry Vs Particle Image Velocimetry. *Applied Optics*, vol. 23, pp. 1690-1691.
- [2] A. H. Khalid and K. Kontis (2008) Thermographic phosphors for high temperature measurements: Principles, current state of the art and recent applications. *Sensors*, vol. 8, pp. 5673-5744.
- [3] P. Neubert (1937) Device for indicating the temperature distribution of hot bodies. (ed) US Patent No. 2,071,471.
- [4] J. E. Parks, J. S. Armfield, T. E. Barber, J. M. E. Storey, and E. A. Wachter (1998) In situ measurement of fuel in the cylinder wall oil film of a combustion engine by LIF spectroscopy. *Applied Spectroscopy*, vol. 52, pp. 112-118.
- [5] A. Omrane, G. Juhlin, F. Ossler, and M. Alden (2004) Temperature measurements of single droplets by use of laser-induced phosphorescence. *Applied Optics*, vol. 43, pp. 3523-3529.
- [6] N. Fuhrmann, T. Kissel, A. Dreizler, and J. Brübach (2011) Gd₃Ga₅O₁₂: Cr—a phosphor for two-dimensional thermometry in internal combustion engines. *Measurement Science and Technology*, vol. 22, pp. 045301.
- [7] B. Fond, C. Abram, A. L. Heyes, A. M. Kempf, and F. Beyrau (2012) Simultaneous temperature, mixture fraction and velocity imaging in turbulent flows using thermographic phosphor tracer particles.

Optics Express, vol. 20, pp. 22118-22133.

- [8] J. Brubach, J. Janicka, A. Dreizler (2009) An algorithm for the characterisation of multi-exponential decay curves, *Optics and Lasers in Engineering*, vol. 47, pp. 75-79.
- [9] A.H. Khalid, K. Kontis (2009) 2D surface thermal imaging using rise-time analysis from laser-induced luminescence phosphor thermometry, *Measurement Science and Technology*, vol. 20, pp. 025305.
- [10] S.J. Yi, H.D. Kim, K.C. Kim (2014) Decay-slope method for 2-Dimensional temperature field measurement using thermographic phosphors, *Experimental Thermal and Fluid Science*, vol. 59, pp. 1-8.